Available online at www.sciencedirect.com

SCIENCE DIRECT®

Polymer 46 (2005) 1759–1765

polymer

www.elsevier.com/locate/polymer

Study of the thermal elimination process of sulphinyl-based PPV precursors by solid state NMR

P. Adriaensens*, H. Roex, D. Vanderzande, J. Gelan[1]

Division Chemistry, Institute for Material Research (IMO), Limburgs Universitair Centrum, Universitaire Campus, Building D, B-3590 Diepenbeek, Belgium

Received 27 August 2004; received in revised form 16 December 2004; accepted 17 December 2004
Available online 21 January 2005

Abstract

A sensitive protocol to judge the completeness of the elimination reaction for soluble and insoluble conjugated polymers prepared via precursor routes is presented based on UV/vis and ^{1}H wideline NMR relaxometry in the solid state. Especially the proton spin–lattice decay time in the rotating frame, $T_{1\rho H}$, has proven to be suitable for an accurate determination of the completeness of the elimination reaction. Especially for long side-chain substituted PPV derivatives, UV/vis seems to be limited due to thermochromic effects. Furthermore, it is shown by solid state ^{2}H wideline NMR spectroscopy that incomplete elimination results in an enhanced polymer backbone chain mobility. Both the completeness of elimination and insight into the molecular dynamics can be of significant importance toward the performance of photovoltaic devices.
© 2004 Elsevier Ltd. All rights reserved.

Keywords: Conjugated polymers; NMR relaxometry; Thermal elimination

1. Introduction

In the field of plastic electronics considerable research has focussed on the synthesis of new conjugated polymers and device improvement (life time, efficiency…), but up to now little is known about the ‘triangular’ relationship between molecular structure (structural defects inherent to the synthetic route)—morphology—device performance. On the other hand this knowledge can be of utmost importance since conjugation defects can heavily influence the final morphology and the opto-electronic properties. Conjugated polymers can be synthesized in a direct way, e.g. via Wittig reactions or Suzuki-coupling. These routes, however, are not so attractive because the resulting polymers have a low degree of solubility and processability. Therefore, high molecular weight conjugated polymers are often synthesized via precursor routes such as the Wessling [1], Gilch [2] and sulphinyl [3] precursor routes, whereby a precursor polymer is converted thermally or chemically toward a conjugated polymer. To obtain a fully conjugated polymer by thermal conversion, control of the elimination temperature and elimination time is a prerequisite since it determines the degree of conversion. If non-eliminated groups remain present, they will act as structural sp^3 defects that disturb not only the conjugation but also the conformation. In this work we opted for MDMO-PPV (poly(2-methoxy-5-(3,7-dimethyloctyloxy)1,4-phenylene vinylene), also called OC$_1$C$_{10}$-PPV), the workhorse of p-type conjugated polymers, that is prepared via the sulphinyl precursor [3] route from a *n*-butylsulphinyl MDMO-PPV precursor polymer since this route allows to isolate a stable precursor polymer. This characteristic allows one to study the thermal elimination step which is depicted in Fig. 1. The thermal elimination reaction is considered to proceed via a *syn*-elimination [4] in which sulphenic acids are expulsed as the double bonds are formed. An additional advantage of MDMO-PPV is that it remains soluble and processable in its conjugated state.

Previous results show a charge carrier mobility in a field effect transistor (FET) prepared with ‘standard’ eliminated MDMO-PPV (i.e. one step elimination in toluene at 110 °C)

---

* Corresponding author. Tel.: +32 11 26 83 12.

E-mail addresses: peter.adriaensens@luc.ac.be (P. Adriaensens), jan.gelan@luc.ac.be (J. Gelan).

[1] Tel.: +32 11 26 83 96; fax: +32 11 26 83 01.

0032-3861/$ - see front matter © 2004 Elsevier Ltd. All rights reserved.
doi:10.1016/j.polymer.2004.12.029

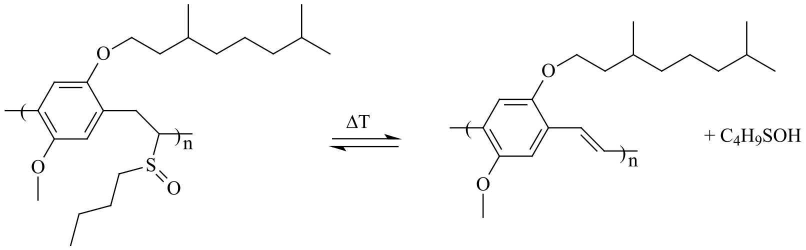

Fig. 1. Scheme of the thermal conversion of the *n*-butylsulphinyl MDMO-PPV precursor polymer towards the conjugated state.

of 2.2×10^{-4} cm^2 V^{-1} s^{-1} as compared to 3.0×10^{-4} cm^2 V^{-1} s^{-1} when a 'two-steps' eliminated MDMO-PPV (i.e. a standard elimination followed by precipitation and repeated reflux in fresh toluene at 110 °C) [5,6] is used. In a previous paper [5], based on quantitative liquid-state ^{13}C NMR of the *n*-butylsulphinyl MDMO-PPV precursor polymer which was ^{13}C-enriched at the olefinic carbons, it was demonstrated that the 'standard' elimination procedure resulted in 7% of non-eliminated sulphinyl groups while this amount could be reduced to less than 1% by the 'two-steps' conversion. This indicates that the charge carrier mobility can be increased by reducing the amount of non-eliminated groups (sp^3 defects). Therefore, the development of a general analytical protocol that allows a fast and sensitive (as compared to ^{13}C NMR) detection of the end phase of the elimination, i.e. whether the semi-conducting polymers are fully conjugated or not, is rather crucial and is the first goal of this work. Such a protocol will even be of more importance for conjugated polymers, which become insoluble in the conjugated state. We, therefore, evaluated the use of in situ UV/vis and proton wideline NMR relaxometry (requires only 5–10 mg of material) in the solid state (the state of the film in the device). It is demonstrated that the spin–lattice relaxation time in the rotating frame, $T_{1\rho\mathrm{H}}$, offers a fast, sensitive and robust criterium to detect the end stage of elimination. The second goal of this study concerns the confirmation of the relationship between the amount of structural sp^3 defects due to incomplete elimination and the molecular chain dynamics as studied by solid state ^{2}H wideline NMR spectroscopy.

2. Experimental section

2.1. Materials

2.1.1. Non-labeled polymers

The *n*-butylsulphinyl-MDMO-PPV precursor polymer was prepared and characterized as described before [7]. The precursor polymer was dissolved in toluene and converted toward the conjugated state by a 'one-step' or 'standard' thermal elimination under an inert atmosphere during 90 min at 70, 80, 90, 100 and 110 °C, respectively. After cooling down to 50 °C, the (partly) conjugated polymers were precipitated in methanol. The 'two-steps' eliminated polymer was obtained by a 'standard' elimination followed by precipitation and repeated reflux in fresh toluene at 110 °C [5]. The ^{13}C-labeled precursor polymer, used to study the elimination for 90 min at 80 °C by means of ^{13}C liquid state NMR, was synthesized analogously to the previous reported synthesis of other ^{13}C-labeled MDMO-PPVs [5].

2.1.2. ^{2}H-labeled monomers and polymers (Fig. 2).

*2.1.2.1. Preparation of 2,5-bis(chloro-^{2}H-methyl)-1-(3,7-dimethyloctyloxy)-4-methoxybenzene **1**.* A 3.26 g (0.012 mol) of *p*-methoxyphenol and 1 g (0.033 mol) of paraformaldehyde-^{2}H (isotopic purity of 99%, Cambridge Isotope Laboratory, Inc., Andover) were placed in a 100 ml three-neck round bottom flask. After adding 6.5 g (0.066 mol) of 37% HCl under N_2, a 12.25 g (0.12 mol) of acetic anhydride was added dropwise at such a rate that the internal temperature did not exceed 70 °C. After stirring for 3.5 h at 75 °C, the mixture was cooled and a light colored solid crystallises at 30 °C. Afterwards, the reaction mixture was admixed with 11 ml of cold-saturated sodium acetate solution, followed by a dropwise addition of 25% NaOH (8 ml). The mixture was heated to 52 °C and subsequently cooled in an ice bath while stirring. The cream-colored solid was filtered off, washed with deuterated water (7 ml) and dissolved in hexane (24 ml). After extraction with deuterated water, the yellowish organic phase was dried over $MgSO_4$, filtered and evaporated. After crystallization, a 3.78 g (87%) of **1** was isolated. Melting point: 65 °C. ^{1}H NMR (300 MHz, $CDCl_3$), δ (ppm) = 6.9 (m, 2H, H_{ar}); 4.0 (m, 2H, OCH_2); 3.8 (s, 3 H, OCH_3); 1.9 (1H); 1.7 (1H); 1.6 (2H); 1.4 (2H); 1.3 (1H); 1.2 (3H); 1.0 (d, J = 6.6 Hz, 3H, CH_3); 0.9 (d, J = 6.7 Hz, 6H; 2×CH_3). ^{2}H NMR (61.5 MHz, $CDCl_3$), δ (ppm) = 4.6 ppm. ^{13}C NMR (100 MHz, $CDCl_3$), δ (ppm) = 19.8 (1C); 22.6 (2C); 24.6 (1C); 27.9 (1C); 30.2 (1C); 36.6 (1C); 37.4 (1C); 39.2 (1C); 41.2 (2C); 56.4 (1C); 67.9 (1C); 113.2 (1C); 114.3 (1C); 127.0 (2C); 151.4(2C). MS (CI, *m/z*, rel.int. (%)): 365 $[M+1]^+$.

*2.1.2.2. Preparation of bis-tetrahydrothiopheniumsalt of 2,5-bis(chloro-^{2}H-methyl)-1-(3,7-dimethyloctyloxy)-4-methoxybenzene **2**.* A solution of 7.8 g (0.02 mol) of **1** and 7.4 g (0.08 mol) of tetrahydrothiophene in MeOD (15 ml)

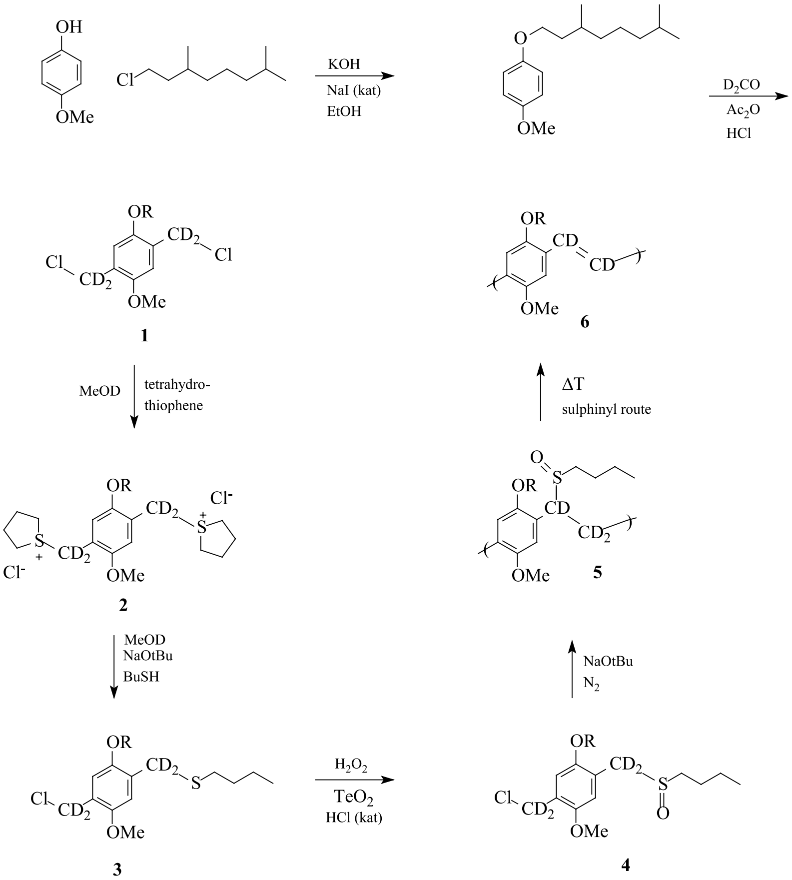

Fig. 2. Synthesis of the deuterated monomers and polymers.

was stirred for 70 h at ambient temperature. After precipitation in aceton (100 ml), the precipitate was washed with hexane. The product (4.9 g, 45%) was dried under reduced pressure at room temperature. ^{1}H NMR (300 MHz, D_2O), δ (ppm) = 7.1 (d, 2H, H_{ar}); 4.0 (m, 2H, OCH_2); 3.8 (s, 3H, OCH_3); 3.4 (m, 8H, $S(CH_2)_2(CH_2)_2$); 2.2 (m, 8H, $S(CH_2)_2(CH_2)_2$); 1.8 (1H); 1.7 (1H); 1.6 (2H); 1.4 (2H); 1.3 (1H); 1.2 (3H); 1.0 (d, $J = 6.6$ Hz, 3H, CH_3); 0.9 (d, $J = 6.7$ Hz, 6H; 2×CH_3). ^{2}H NMR (61.5 MHz, D_2O), δ (ppm) = 4.2 ppm. ^{13}C NMR (100 MHz, D_2O), δ (ppm) = 21.3 (1C); 24.31/24.39 (2C); 26.4 (1C); 29.6 (1C); 30.7 (1C); 31.3 (1C); 37.6 (1C); 38.7 (1C); 40.9 (1C); 43.9 (2C); 45.5 (1C); 58.6 (1C); 70.0 (1C); 117.8/118.6 (2C); 121.9/122.4 (2C); 153.7/154.3 (2C).

*2.1.2.3. Preparation of 2-((^{2}H-butylsulphanyl)methyl)-5-(^{2}H-chloromethyl)-1-(3,7-dimethyloctyloxy)-4-methoxybenzene **3**.* A mixture of NaOtBu (0.86 g, 8.9 mmol) and *n*-butanethiol (0.8 g, 8.9 mmol) in MeOD (20 ml) was stirred for 30 min at room temperature. The clear solution was added in one portion to a stirred solution of **2** (4.9 g, 8.9 mmol). After 1 h the reaction mixture was neutralized with aqueous HCl, if necessary, and concentrated in vacuo. The crude product was diluted with $CHCl_3$ (21 ml), the precipitate was filtered off and the solvent was evaporated. The obtained oil was diluted with petroleumether (boiling range 100–140 °C) and concentrated to remove the tetrahydrothiophene. This sequence was repeated three times to afford a light yellow viscous oil. A 3.7 g (8.9 mmol) of crude product was formed. ^{1}H NMR (300 MHz, $CDCl_3$), δ (ppm) = 6.89/6.87 (d, 2H, H_{ar}); 4.0 (m, 2H, OCH_2); 2.5 (m, 2H, $SCH_2(CH_2)_2CH_3$); 1.9–1.2 (14H, $H_{alif.}$); 1.0 (3H, CH_3); 0.9 (9H, 3×CH_3). ^{2}H NMR (61.5 MHz, $C_2D_2Cl_4$), δ (ppm) = 4.6 (–CD_2Cl); 4.0/3.8 (–CD_2SR). MS (CI, *m/z*, rel.int. (%)): 421 $[M+1]^+$.

*2.1.2.4. Preparation of 2-(^{2}H-butylsulphinyl)methyl)-5-(^{2}H-chloromethyl)-1-(3,7-dimethyloctyloxy)-4-methoxybenzene **4**.* An aqueous (35 wt%) solution of H_2O_2 (1.3 g, 13.4 mmol) was added dropwise to a solution of crude thioether **3** (8.9 mmol), TeO_2 (0.17 g, 1.1 mmol) and three drops of concentrated HCl in 1,4-dioxane (34 ml). The reaction was followed on TLC (time: 2.5 h) and as soon as overoxidation took place, it was quenched by a saturated aqueous NaCl solution (30 ml). After extraction with $CHCl_3$ (3×30 ml), the organic layers were dried over $MgSO_4$ and concentrated in vacuo. The reaction mixture was purified by column chromatography (SiO_2, eluent hexane/ethylacetate 60/40) to give pure **4** (1.74 g, 65%) as a light yellow viscous oil. ^{1}H NMR (300 MHz, $CDCl_3$), δ (ppm) = 6.9 (d, 1H, H_{ar});

6.8 (d, 1H, H_{ar}); 4.3/4.1 + 3.8/3.6 (dd, 2H, $^{1}J = 130$ Hz, $CH_2S(O)R$); 3.9 (m, 2H, OCH_2); 3.8 (s,3H, OCH_3); 1.9 (1H); 1.7 (1H); 1.6 (2H); 1.4 (2H); 1.3 (1H); 1.2 (3H); 1.0 (d, $J = 6.6$ Hz, 3H, CH_3); 0.9 (d, $J = 6.7$ Hz, 6H; $2\times CH_3$). ^{2}H NMR (61.5 MHz, $C_2D_2Cl_4$), δ (ppm) = 4.6 ($-CD_2Cl$); 4.0/3.8 ($-CD_2SR$). ^{13}C NMR (100 MHz, $CDCl_3$), δ (ppm) = 13.5 (1C); 19.8 (1C); 22.1 (1C); 22.6 (2C); 24.6 (2C); 27.9 (1C); 30.2 (1C); 36.6 (1C); 37.4 (1C); 39.2 (1C); 41.3 (1C); 49.7 (1C); 52.5 (1C); 56.4 (1C); 67.9 (1C); 112.8 (1C); 115.7 (1C); 119.7 (1C); 127.0 (1C); 151.4 (2C). MS (CI, *m/z*, rel.int. (%)): 437 $[M+1]^{+}$. The preparation and the thermal conversion of the deuterated precursor polymer of 2-(^{2}H-butylsulphinyl)methyl-5-(^{2}H-chloromethyl)-1-(3,7-dimethyloctyloxy)-4-methoxybenzene (**5** + **6**) is accomplished as reported for the non-labeled polymers.

2.2. Analytical techniques

2.2.1. In situ ultraviolet visible spectroscopy

The in situ UV/vis spectra were recorded on a Cary 500 UV–vis–NIR spectrophotometer (interval 1 nm, scan rate 600 nm/min, continuous run from 200 to 800 nm). The *n*-butylsulphinyl MDMO-PPV precursor polymer was spin-coated from a chloroform solution (6 mg/ml) on a quartz disc (diameter 25 mm, thickness 3 mm) at 1000 rpm. A non-isothermal heating experiment with a ramp of 2 °C/min and starting from ambient temperature up to 300 °C was carried out under a continuous flow of nitrogen in a Harrick high temperature cell (Safir).

2.2.2. NMR spectroscopy

2.2.2.1. ^{1}H wideline NMR. All proton wideline NMR measurements were carried out on a Varian Unity 400 spectrometer in a 5 mm coil of a dedicated wideline probe at room temperature and 65 °C. The temperature at the specimen was calibrated by means of the frequency difference between the resonances of ethyleneglycol. A spectral width of 2 MHz was used and a preparation delay of five times the T_{1H} relaxation time was always respected between successive accumulations. The $T_{1\rho H}$ decay times were measured by applying a spin-lock field (45 kHz) of variable duration after the initial $90°_{x'}$ pulse of a solid echo pulse sequence ($90°_{x'}$–spin-lock–$\tau/2$–$90°_{y'}$–$\tau/2$–acquire). The $T_{1\rho H}$ decay times were analyzed by a sum of two exponentials $M(t) = \sum M_{0,j} \exp(-t_i/T_{1\rho H,j})$ in which t_i is the variable spin-lock time. Data were analysed by non-linear least squares fitting methods employing the Levenberg–Marquardt algorithm [8] of the programme Origin 6.1.

2.2.2.2. ^{2}H wideline NMR. ^{2}H NMR line shape spectra were obtained as a function of temperature on the same spectrometer at 61.5 MHz using the quadrupolar echo pulse sequence ($90°_{x'}$–$\tau/2$–$90°_{y'}$–$\tau/2$–acquire) with a pulse length of 2 μs, 600 accumulations, a total echo delay of 22 μs (echo maximum) and a preparation delay of 3 s.

3. Results and discussion

3.1. Ultraviolet visible spectroscopy

In situ UV–vis spectroscopy is a fast analytical technique by which the formation of the conjugated system (red shift of λ_{max}) can be followed as a function of temperature. Fig. 3 shows a series of UV–vis absorption spectra of a *n*-butylsulphinyl MDMO-PPV precursor polymer film (further referred to as precursor polymer) recorded at increasing temperatures. Initially the absorption band at 301 nm, originating from the precursor polymer, decreases upon increasing the temperature, while a new absorption band at 374 nm arises due to the formation of rather short conjugated sequences. The latter disappears as the elimination reaction proceeds, while a new and broad absorption band is formed at longer wavelengths. This absorption band clearly shows a red shift upon increasing the elimination temperature, indicating that the effective conjugation length of the conjugated π-system increases and reaches a maximum absorbance around 475 nm (λ_{max}) at 110 °C. Above 110 °C, however, a blue shift can be noticed due to a 'thermochromic effect': a change of the average torsion angles due to an increase of the molecular chain dynamics by heating. This will lead to deviations in the coplanarity between the phenyl rings and double bonds and consequently to a decrease in λ_{max}. For this polymer the thermochromic process is reversible to about 220 °C as can be demonstrated by several heating–cooling experiments at different temperatures [9].

From these in situ UV/vis experiments, we can conclude that the elimination reaction of the precursor polymers gradually proceeds in the temperature range between 70 and 110 °C (Fig. 3). Unfortunately, due to the competition between the growing conjugated system (increase in λ_{max}) and the thermochromic effect (decrease in λ_{max}), in situ

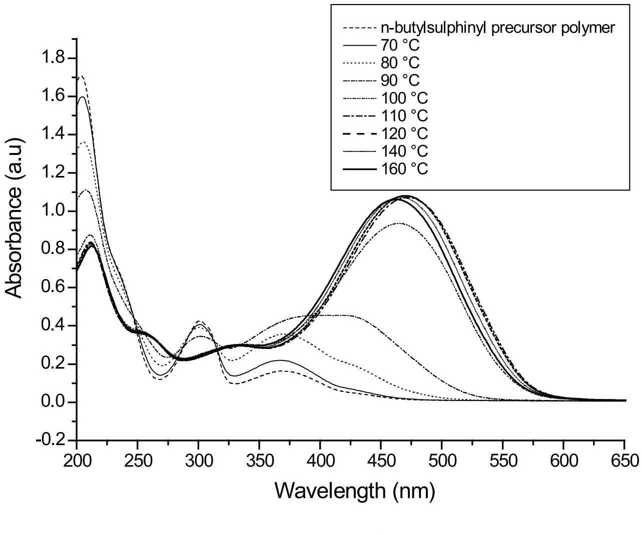

Fig. 3. In situ UV–vis absorption spectra of the *n*-butylsulphinyl MDMO-PPV precursor polymer as a function of temperature.

UV/vis spectroscopy becomes less sensitive toward the detection of the end state of the thermal elimination. This phenomenon has already been described [10] and is recently also observed for PPV derivatives of which the phenyl ring bears one or more long side-chains [9,11]. It is assumed that the thermochromic effect is related to the T_g of the polymers since its appearance at relative low temperatures might be explained by the low T_g of these substituted polymers (about 34 °C for the *n*-butylsulphinyl MDMO-PPV precursor polymer and about 55 °C for the conjugated MDMO-PPV polymer). Although such long side-chains seem to limit an accurate detection of the end state of elimination by in situ UV/vis, they are usually preferred to ensure the solubility and processability of semi-conducting polymers in the conjugated state toward device fabrication.

3.2. ^{1}H wideline solid state NMR relaxometry

^{1}H-wideline solid state NMR is another fast analytical technique (in the order of minutes) that offers the possibility to study the molecular chain mobility and morphology on the nanometer scale by means of a diverse set of relaxation decay times. The relaxation times of interest are the proton spin–lattice relaxation time in the laboratory and the rotating frame, T_{1H} and $T_{1\rho H}$, respectively, and the proton spin–spin relaxation time, T_{2H}. The different relaxation times are affected by molecular motions within a certain frequency range. The T_{1H} decay time (in the order of seconds) is dominated by the spectral density of motions in the MHz region and is often determined by mobile side-chain or end group motions. The $T_{1\rho H}$ decay time (in the order of milliseconds) is affected by motions in the kHz region and is suitable for studying the polymer backbone motions. For rigid systems, the T_{2H} relaxation time (in the order of microseconds) is a local probe which is mainly determined by the strength of local fields.

In this study, precursor polymers were eliminated at 70, 80, 90, 100 and 110 °C during 90 min in solution according to the 'standard' elimination procedure. Afterwards the relaxation times were measured at room temperature (below T_g) and at 65 °C (slightly above the T_g of the conjugated polymers). The $T_{1\rho H}$ relaxation decay time seems to be a robust parameter to study the progression of the elimination, i.e. the stiffening of the polymer backbone, while the T_{1H} and T_{2H} decay times were much less sensitive (results not shown). This can easily be explained by the fact that the backbone motions (in the order of kHz) are situated intermediate with respect to the motional regimes to which T_{1H} and T_{2H} are sensitive. The ^{1}H-spectra of all polymers clearly show a Lorentzian lineshape superimposed on a broader Gaussian lineshape. The free induction decay (FID) indeed has to be analysed by a combination of a Lorentzian and Gaussian function to describe the T_2 relaxation. The $T_{1\rho H}$ relaxation behaves biexponentially, resulting in a short ($T^{S}_{1\rho H}$) and long ($T^{L}_{1\rho H}$) decay time, with proton fractions of about 25 and 75%, respectively. It is, however, difficult to describe the origin of this biexponential behaviour due to unknown contributions of the long side chains and of the process of spin diffusion. The latter can obstructs a straightforward interpretation of variable temperature data since its contribution will vary strongly with temperature in the region around the glass transition (T_g) of the polymer.

Concerning the $T_{1\rho H}$ measurements at room temperature, it was found that both decay times are quasi independent on the progression of the elimination reaction ($T^{S}_{1\rho H}$ and $T^{L}_{1\rho H}$ remain around 1.2 and 3.3 ms, respectively). On the other hand the $T_{1\rho H}$ experiments at 65 °C (slightly above T_g; Fig. 4) show, especially for $T^{L}_{1\rho H}$, a significant increase upon increasing the elimination temperature. In agreement with the UV/vis measurements, this increase in $T^{L}_{1\rho H}$ is most pronounced between 90 and 100 °C, indicating a huge progress in the length of conjugation and related backbone molecular dynamics (Figs. 3 and 4). Notice that the evolution of the $T^{S}_{1\rho H}$ decay time shows the same behaviour but on a different axis scaling.

These observations are further confirmed by quantitative liquid-state ^{13}C NMR spectra recorded for a *n*-butylsulphinyl MDMO-PPV precursor polymer which is selectively ^{13}C-labeled (the carbon atoms of the double bond to be formed) and thermally eliminated under different experimental conditions. Liquid-state ^{13}C NMR demonstrates a degree of elimination of 44% for a precursor polymer which is eliminated for 90 min at 80 °C. Previous ^{13}C NMR experiments [5] showed that after 'standard' elimination at 110 °C, still 7% of non-eliminated sulphoxide groups were present. This amount could be reduced to 2% by increasing the elimination temperature to 170 °C. However, by performing a 'two-steps' elimination procedure at 110 °C an almost fully conjugated MDMO-PPV with less than 1% of non-eliminated groups was already obtained. This can be

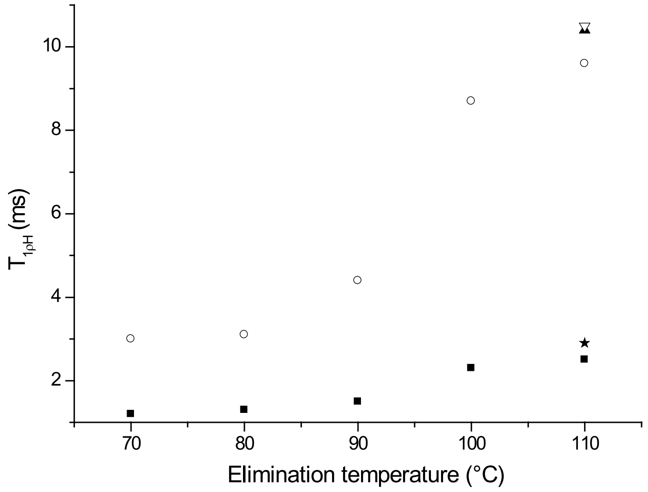

Fig. 4. The $T_{1\rho H}$ decay times measured at 65 °C as a function of the elimination temperature for 'standard' eliminated MDMO-PPV ($T^{S}_{1\rho H}$ (■) and $T^{L}_{1\rho H}$ (○)), 'two-steps' eliminated MDMO-PPV ($T^{S}_{1\rho H}$ (★) and $T^{L}_{1\rho H}$ (▲)) and 'three-steps' eliminated MDMO-PPV ($T^{L}_{1\rho H}$ (▽)).

explained by a displacement of the equilibrium towards the conjugated polymer upon removing the eliminated reaction products (Fig. 1). These experiments clearly demonstrate that the amount of non-eliminated groups (structural sp^3 defects) is strongly dependent on the elimination temperature and elimination procedure (time duration has no effect above 45 min). The $T_{1\rho H}^{L}$ decay time of a 'two-steps' eliminated MDMO-PPV can, therefore, be considered as representatives for the fully conjugated system. Fig. 4 indeed shows that the $T_{1\rho H}^{L}$ decay time is still very sensitive in detecting this final phase of elimination (disappearance of the last 7% of non-eliminated groups): measured at 65 °C the value of $T_{1\rho H}^{L}$ is significantly longer for the 'two-steps' eliminated polymer as compared to this found for the 'standard' eliminated polymer. This indicates a further change in the polymer backbone dynamics and is fully in agreement with the ^{13}C liquid NMR results. These findings might (partly) explain the differences in charge carrier mobility as mentioned in the introduction. This in contrast with UV/vis measurements at room temperature on films prepared from polymers which were eliminated in solution via the 'standard' and 'two-steps' elimination procedure and for which no further difference in λ_{max} could be observed (Fig. 5). To confirm the completeness of conjugation for the'two-steps' eliminated polymer, a 'three-steps' eliminated polymer was examined. Fig. 4 clearly shows that the $T_{1\rho H}^{L}$ decay time measured for this polymer coincides completely with the value found for the 'two-steps' eliminated polymer, confirming the completeness of elimination.

This information allows us to propose a fast and sensitive measuring procedure to judge the end state of elimination for precursor-based conjugated polymers. To start with, a suitable elimination temperature can be quickly selected based on in situ UV/vis measurements. For soluble polymers, which can still be processed after the thermal elimination, the $T_{1\rho H}^{L}$ decay times can then be determined after a 'standard' and a 'two-steps' elimination procedure. As long as $T_{1\rho H}^{L}$ remains dependent on the elimination procedure, elimination is not complete and additional elimination steps have to be carried out or the elimination temperature has to be raised. In case of insoluble conjugated polymers (without long side-chains) which have to be eliminated after processing, i.e. in film, $T_{1\rho H}^{L}$ measurements allow to determine the optimal elimination temperature (and time).

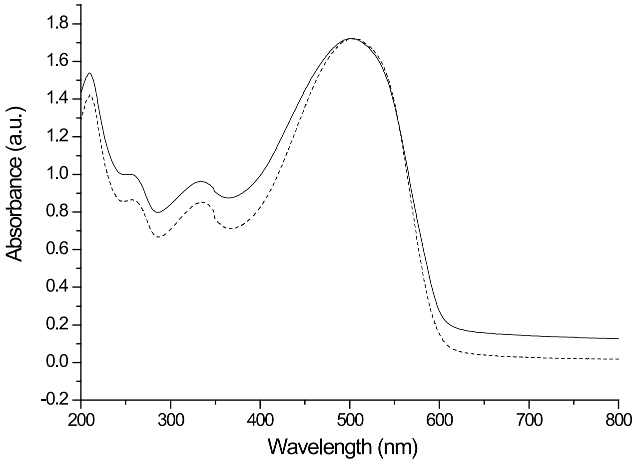

Fig. 5. Solid state UV–vis spectra of a 'standard' (solid line) and a 'two-steps' (dotted line) eliminated polymer recorded on films at room temperature.

In the next part, the influence of incomplete elimination (structural sp^3 defects) on the polymer backbone dynamics is demonstrated by means of solid state ^2H NMR experiments performed on a 'standard' (7% non-eliminated groups) and a 'two-steps' eliminated ($<1\%$ non-eliminated groups) MDMO-PPV of which the double bonds are ^2H-labeled.

3.3. ^2H wideline NMR spectroscopy

Solid state ^2H wideline NMR spectroscopy can provide insight into the molecular dynamics of polymers. Solid state deuterium NMR has already contributed to a better understanding of the properties of PPV: ^2H resonance line shapes of both unstretched and stretched phenylene ring-deuterated PPV (PPV-d_4) have shown that portions of the PPV chains undergo 180° rotational jumps about the 1,4 ring axis ('ring flips') at elevated temperatures [12]. Spectra of vinylene-deuteraded PPV (PPV-d_2) obtained at elevated temperature reveal substantial chain motions which are consistent with 180° rotational jumps of portions of the PPV chain about the crystallographic *c*-axis [13].

The influence of various amounts of structural sp^3 defects on the molecular dynamics of MDMO-PPVs was examined as a function of temperature. The synthesis of the deuterated MDMO-precursor PPV is described in the experimental part. Since the 'standard' as well as the 'two-steps' conjugated polymer (MDMO-PPV-d2 of which 99.5% of the vinylene carbons are deuterated) are derived from the same precursor, contributions due to differences in molecular weight and so amount of end groups can be excluded. Fig. 6(a) and (b) show the changes in deuterium line shape as a function of temperature for the 'standard' and 'two-steps' eliminated polymers, respectively. Broad Pake patterns resulting from static, random orientations of the C–D bonds are observed at low temperatures and show a quadrupolar splitting, $\Delta\upsilon_q$, of 128 kHz. Upon increasing the temperature from 20 to 140 °C in steps of 15 °C, the Pake pattern slightly changes into a shape which represents (partial) motional averaging of the quadrupolar interaction. Notice already that, in the center of the Pake pattern, a sharp resonance line appears at lower temperatures for the 'standard' eliminated polymer (80 °C) as compared to the 'two-steps' eliminated polymer (95 °C). This central resonance can be attributed to fast isotropic motions around the structural sp^3 defects.

Below the glass-transition temperature, however, the

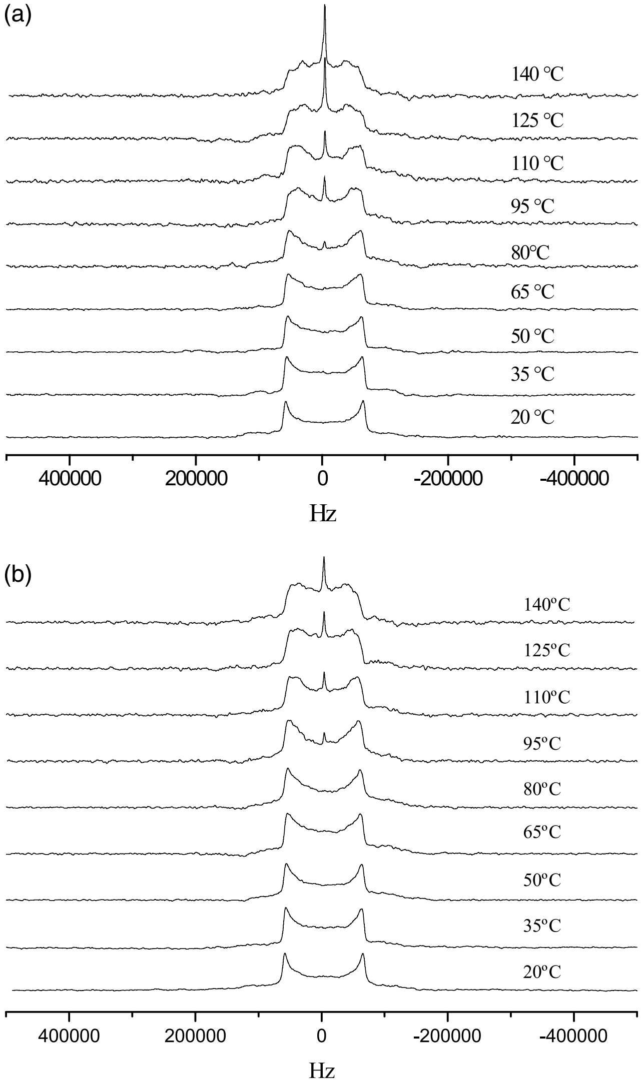

Fig. 6. ^{2}H NMR spectra of 'standard' (a) and 'two-steps' (b) eliminated MDMO-PPV as a function of temperature.

polymer is vitrificated explaining the absence of the isotropic line at low temperatures. At elevated temperatures and due to a more pronounced conformational freedom around the numerous sp^3 defects, the central sharp resonance line appears already at lower temperatures for the 'standard' eliminated polymer as compared to the 'two-steps' eliminated polymer. These experiments clearly confirm the influence of the degree of elimination on the polymer backbone chain dynamics.

4. Conclusion

In this paper, a fast and sensitive protocol is presented to determine the end state of the elimination reaction for conjugated polymers based on solid state ^{1}H wideline NMR. The slow decaying time constant of the proton spin–lattice relaxation time in the rotating frame, $T^{\mathrm{L}}_{1\rho\mathrm{H}}$, seems to be very sensitive towards the detection of changes in the backbone chain dynamics upon elimination. The extended conjugation length of the 'two-steps' eliminated polymer might explain the higher charge carrier mobility observed in photovoltaic devices. In addition, ^{2}H wideline experiments have confirmed the enhancement in backbone chain dynamics with increasing amounts of non-eliminated groups (structural sp^3 defects).

Acknowledgements

The authors gratefully acknowledge The Fund for Scientific Research-Flanders (FWO) and the Belgian Programme on Interuniversity Attraction Poles (IUAP), initiated by the Belgian State Prime Minister's Office, for the financial support. We also want to thank the IWT (Institute for the Promotion of Innovation by Science and Technology in Flanders) for the financial support via the SBO-project 030220 'Nanosolar'.

References

[1] Wessling RA. J Polym Sci, Polym Symp 1985;72:55.
[2] Gilch HG, Wheelwright WL. J Polym Sci A 1966;4:1337.
[3] Issaris A, Vanderzande D, Gelan J. J Polym 1997;38:2571.
[4] (a) Kwart H, George TJ, Louw R, Ultee W. J Am Chem Soc 1978;3927.
    (b) Janssen JWAM, Kwart H. J Org Chem 1977;42:1530.
[5] Roex H, Adriaensens P, Vanderzande D, Gelan J. Macromolecules 2003;36(15):5613.
[6] Munters T. PhD Dissertation, Limburgs Universitair Centrum, Diepenbeek; 2004.
[7] Van Breemen A, De Kok M, Adriaensens P, Gelan J, Vanderzande D. J Org Chem 1999;64:3106.
[8] Marquardt DW. J Soc Ind Appl Math 1965;431.
[9] Kesters E, Lutsen L, Vanderzande D, Gelan J, Nguygen TP, Molinié P. Thin Solid Films 2002;120:403.
[10] Nobuaki H, Naoki H, Shigehiro M. Synth Met 1996;80:67.
[11] Motmans F. PhD Dissertation, Limburgs Universitair Centrum, Diepenbeek; 2004.
[12] (a) Simpson JH, Egger N, Masse MA, Rice DM, Karasz FE. J Polym Sci, Part B: Polym Phys 1990;28:1859.
    (b) Simpson JH, Rice DM, Karasz FE. J Polym Sci, Part B: Polym Phys 1992;30:11.
[13] Simpson JH, Liang W, Rice DM, Karasz FE. Macromolecules 1992; 25:3068.